*American Journal of Physics and Applications*
2025, Vol. 13, No. 5, pp. 125-133
https://doi.org/10.11648/j.ajpa.20251305.12

Research Article

# Numerical Investigation of Propagation Characteristics of TE Waves Incident Obliquely to Reentry Plasma Sheath with Bi-Gaussian Electron Density Profile Based on SMM

**Chol-Su Kim[1], Yong-Su Han[1,*], Myong-Il Ri[1], Il-Guk Kim[1], Se-Chol Pak[2]**

[1]Faculty of Physical Science, Kim Chaek University of Technology, Pyongyang, Democratic People's Republic of Korea
[2]Department of Physics, SinUiJu Cha Kwang Su University of Education, Sinuiju, Democratic People's Republic of Korea

## Abstract

The analysis of the propagation characteristics of electromagnetic wave in reentry plasma layer is an important issue in fields of spacecraft control, communication and stealth technology, which has attracted the attention of many researchers in last decades. In this paper, the propagation characteristics of obliquely incident TE waves into reentry plasma sheath with bi-Gaussian electron density profile are investigated by using the scattering matrix method (SMM). Based on the matching condition of electromagnetic wave (EM) in multilayer plasmas, the scattering matrix equations of the oblique-incident TE waves are derived and the reflection, transmission and absorption characteristics with incident angle, plasma electron density distribution, and collision frequency are respectively studied. The computational results showed that the reflectance, transmittance, and absorptance change significantly with the incident angle, electron density profile, and collision frequency when the TE wave propagates obliquely into the plasma sheath. In addition, the higher the frequency, the more the reflection vibrations are, and the transmittance and the absorptance peaks move from low to high frequencies with increasing incidence angle, electron density profile and collision frequency. The present method and results may contribute to establish an alternate methodology to overcome the communication blackout by plasma formed around the vehicle during reentry into atmosphere.

## Keywords

S-polarization, Electromagnetic Wave, Plasma Sheath, Scattering Matrix Method, Propagation Characteristics

## 1. Introduction

When a vehicle reenters the Earth's atmosphere at hypersonic speeds, the tremendous heat due to friction with the atmosphere causes the surrounding air molecules to dissociate and ionize, and then, the surface of the hypersonic vehicle would be surrounded by a plasma space sheath [1, 2]. The EM waves radiated from an onboard antenna are largely attenuated by reflection and absorption effects of the plasma sheath, and intermittent communication outage and blackout problem are frequently generated by the plasma sheath [3]. Hence, the study on the interaction mechanism between the

*Corresponding author: hys66815@star-co.net.kp (Yong-Su Han)

**Received:** 1 September 2025; **Accepted:** 13 September 2025; **Published:** 31 October 2025

EM wave and the plasma sheath is of significant importance [4, 5].

Many studies on the propagation characteristics of EM waves in the plasma sheath have been done. In Refs. [6] and [7], there have been researched the absorption, reflection and transmission of EM waves by a nonuniform plasma slab under the different plasma conditions such as center plasma density and collision frequency, and the uniform external magnetic fields. The authors calculated the reflection and absorption power of each subslab by using Fresnel's law and obtained the total reflection power. Applying the impedance transformation method with multilayer dielectrics, Yuan *et al.* [8–9] calculated the reflection power of EM wave and investigated the effects of different plasma parameters and incident wavebands for the total reflection and the absorption, in a bounded plasma stealth model. Hu *et al.* [10] introduced the scattering matrix method (SMM) to calculate the reflection, absorption, and transmission for a nonuniform plasma slab. They divided the nonuniform magnetized plasma slab into a number of subslabs with constant electron densities, and recursively obtained the reflected, absobed and transmitted powers of EM wave. Lu ś *et al.* [11] experimentally measured the propagation signal attenuation in a plasma wind tunnel using the Ka band antenna. Gregoire *et al.* [12] and Cao *et al.* [13] investigated the EM wave's reflection and absorption characteristics of conductive targets coated with nonuniform plasma by using the Wentzel-Kramers-Brillouin (WKB) method. By using Finite-difference time-domain (FDTD) and transmission line methods, Ji *et al.* [14] analyzed the absorption and transmission characteristics of nonuniform plasma layer with varying electron number density of the parabolic profile, and studied functional dependence on the electron number density and collision frequency. Sun *et al.* [15] calculated the back scattering radar cross section with the Runge-Kutta Exponential Time Differencing-Finite Difference Time Domain method to illustrate the strong penetration of terahertz wave. Most of the articles were aimed at the determination of the absorption, reflection and transmission of the vertically incident EM waves in the plasma sheath.

However, the researches on the propagations of the obliquely incident EM waves in the reentry plasma sheath have not been given much attention, and there have been made only a few studies on it. Laroussi *et al.* [16] studied the propagation of microwave launched at an arbitrary angle into magnetized, steady-state, two dimensional, nonuniform and collisional plasma slab in consideration of the condition of continuity of wave impedance at the boundary between subslabs. Cheng *et al.* [17] analyzed both the propagation properties of S-polarization and P-polarization EM waves with the incident angle in inhomogeneous plasmas, by using the direct finite-difference method (DFDM). Numerical results show that the transmittance and reflectance for S-polarization EM wave respectively decrease and increase monotonously with incident angle in plasma with certain collision frequency, and for low-collision plasma, enhanced power absorption can be achieved by P-polarization wave with proper obliquely incident angle. Bai *et al.* [18] studied the transmission properties of the perpendicular polarized wave and the parallel polarized wave obliquely incident in the reentry plasma sheath by using the transmission line analogy (TLA). They calculated the effects of reentry plasma sheath on the polarization property of obliquely incident EM waves for the GPS navigation right hand circularly polarized wave. Mao *et al.* [19] analyzed the propagation characteristics of THz waves in the plasma sheath and proposed the communication frequency with the flight speed.

In the paper, we discuss the propagation characteristics of obliquely incident TE wave in the reentry plasma sheath, by employing the SMM. The plasma sheath is considered a nonuniform, unmagnetized, cold, weakly ionized, steady state, and collisional. We examine the effects of the incident angle, plasma density profile and collision frequency for the reflectance, transmittance and absorptance of obliquely incident TE wave in the reentry plasma sheath.

This paper is organized as follows. Section 2 outlines an approximate layered model for the nonuniform reentry plasma sheath, presents a modified computation method for TE waves obliquely propagating in the plasma sheath, and verifies the validity and the precision of the model. In Section 3, the numerical method is used to study the propagation characteristics of obliquely incident TE waves in our plasma model, and the reflectance, transmittance and absorptance for the incident wave are drawn with various incident angles, electron densities, and collision frequencies. The conclusion is mentioned in Section 4.

## 2. Model and Formulation

### 2.1. Physical Model for Plasma Sheath

The electron density distribution of reentry plasma sheath is inhomogeneous and varies with altitude [20]. As shown in Figure 1, the variation of an electron density outward from the vehicle surface at an antenna location can be represented by a bi-Gaussian function [21, 22].

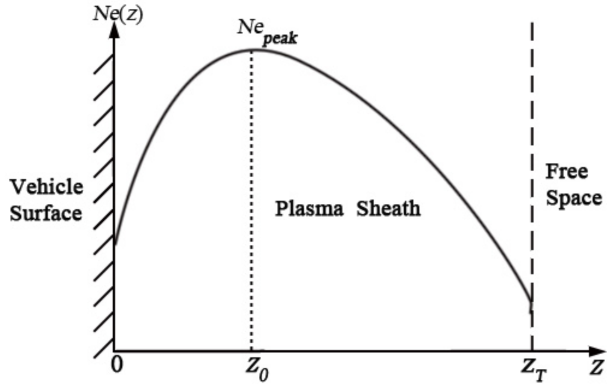


***Figure 1.*** *Variation of an electron density outward from the vehicle surface.*

It is described as follows:

$$Ne(z)=\begin{cases} Ne_{\text{peak}}\exp\left[-a_1(z-z_0)^2\right] & (0\le z<z_0) \\ Ne_{\text{peak}}\exp\left[-a_2(z-z_0)^2\right] & (z_0\le z\le z_{\text{T}}) \end{cases} \tag{1}$$

where $Ne(z)$ is the plasma electron density at distance $z$, $Ne_{\text{peak}}$ is the maximum electron density of the plasma sheath, $z_{\text{T}}$ is the thickness of the plasma sheath, $a_1$ and $a_2$ are the raise index of electron density from the surface wall and the fall-off index to the free space side, respectively, and $z_0$ is the distance from the vehicle surface to the maximum electron density position of the plasma sheath.

## 2.2. Formulations

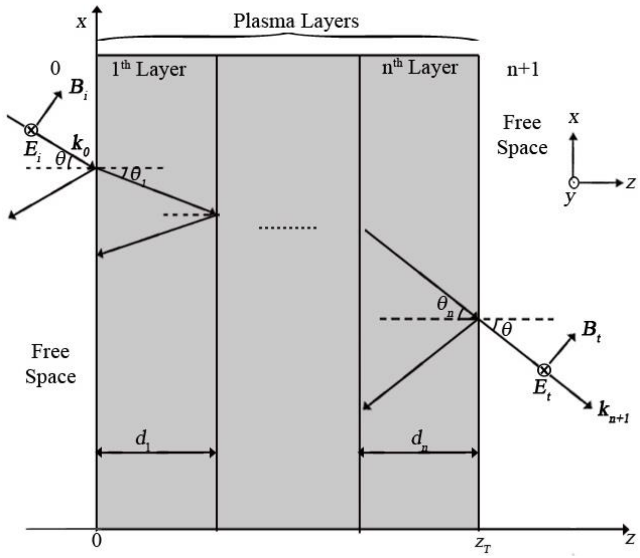


*Figure 2. Propagation schema of obliquely TE waves in the multi-layered plasma.*

The geometry of an obliquely incident TE wave propagating in plasma sheath of the *xoz* plane is shown in Figure 2. The electron density distribution of plasma sheath varies only in *z*-axis direction. The plasma sheath is divided into $n$ sufficiently thin and adjacent layers with constant electrons, that is, we assume that the electron density of plasma in each stratified layer is homogeneous. The complex dielectric function of $m$-th plasma layer given by Drude model [23] has the following form.

$$\varepsilon_{r,m}=1-\frac{\omega_{p,m}^2}{\omega(\omega-j\nu)} \tag{2}$$

where $j=\sqrt{-1}$, $\nu$ is the collision frequency between electron and neutral gas, $\omega$ is the angle frequency of the incident EM wave, $\omega_{p,m}=\sqrt{\left(e^2Ne_m\right)/\left(m_e\varepsilon_0\right)}$ is the electron plasma frequency, $Ne_m$ is an electron density of $m$-th plasma layer, $\varepsilon_0$ is the permittivity of free space, $e$ and $m_e$ are the element charge and the mass of electron, respectively.

The EM wave propagating through the $m$-th plasma layer satisfies following Maxwell's equation,

$$\nabla\times\boldsymbol{E}=-\mu_0\frac{\partial\boldsymbol{H}}{\partial t} \tag{3}$$

$$\nabla\times\boldsymbol{H}=\varepsilon_0\varepsilon_{r,m}\frac{\partial\boldsymbol{E}}{\partial t} \tag{4}$$

where $\mu_0$ is the permeability of free space. Eliminating $H$ from these equations, we can obtain as following.

$$\Delta\boldsymbol{E}=\varepsilon_0\mu_0\varepsilon_{r,m}\frac{\partial^2\boldsymbol{E}}{\partial t^2} \tag{5}$$

In the case of TE wave, considering that the solution of the equation (5) have the forms $\boldsymbol{E}=\left(0,\,E_y,\,0\right)e^{j\omega t}$ and $\boldsymbol{H}=\left(H_x,\,0,\,H_z\right)e^{j\omega t}$, and the propagation constant vector is $\boldsymbol{k}=\left(k_x,\,0,\,k_z\right)$, we can obtain $E_y$, i.e.

$$E_y=E(x,z)e^{-jk_zz}e^{-jk_xx} \tag{6}$$

The total electric field in incident region can be written as

$$E_{y,0}=E_0\left(e^{-jk_{z,0}z}+re^{jk_{z,0}z}\right)e^{-jk_{x,0}x} \tag{7}$$

where $r$ is the amplitude reflection coefficient, and $k_{x,0}$ and $k_{z,0}$ are respectively the $x$- and $z$-components of the propagation constant vector in the free space.

In the $m$-th layer, the total electric field is sum of the reflected and incident components, i.e.

$$E_{y,m}=E_0\left(B_me^{-jk_{z,m}z}+C_me^{jk_{z,m}z}\right)e^{-jk_{x,m}x} \tag{8}$$

where, $B_m$ and $C_m$ are unknown coefficients, which are related to transmission and reflection waves in $m$-th layer, and $k_{x,m}$ and $k_{z,m}$ are respectively the $x$- and $z$- components of the propagation constant vector in $m$–th layer as

$$k_{x,m}=k_m\sin\theta_m=k_0\sin\theta \tag{9}$$

$$k_{z,m}=k_m\cos\theta_m \tag{10}$$

where $k_m$ is the complex propagation constant of $m$-th layer as:

$$k_m^2 = \varepsilon_{r,m} \frac{\omega^2}{c^2}, \quad (11)$$

and $c = (\varepsilon_0 \mu_0)^{-1/2}$ is the velocity of light in the free space. According to Snell's law,

$$k_0 \sin\theta = k_1 \sin\theta_1 = \cdots = k_m \sin\theta_m = \cdots = k_n \sin\theta_n \quad (12)$$

where $n$ is a divided number of plasma sheath.

In the last region i. e. $n$+1-th layer, there is only a transmitted wave, thus, the electric field can be expressed as

$$E_{y,n+1} = E_0 \left( t e^{-jk_{z,n+1} z} \right) e^{-jk_{x,n+1} x} \quad (13)$$

where $t$ is the amplitude transmission coefficient.

Applying the matching boundary condition that the tangential components of electric field and its derivations have matched at the each interface [24], we can obtain a matrix equation at $z$=0,

$$\begin{pmatrix} B_1 \\ C_1 \end{pmatrix} = \mathbf{S}_1 \begin{pmatrix} r \\ 1 \end{pmatrix}, \quad (14)$$

where $S_1$ is the scattering matrix of first interface, i.e. interface between free space and plasma sheath, which is defined as

$$\mathbf{S}_1 = \frac{1}{2k_{z,1}} \begin{pmatrix} k_{z,1} - k_{z,0} & k_{z,1} + k_{z,0} \\ k_{z,1} + k_{z,0} & k_{z,1} - k_{z,0} \end{pmatrix}. \quad (15)$$

Considering the matching boundary condition at $m$-th interface ($m \neq 1$), the resulting equation is following,

$$\begin{pmatrix} B_m \\ C_m \end{pmatrix} = \mathbf{S}_m \begin{pmatrix} B_{m-1} \\ C_{m-1} \end{pmatrix}, \quad (16)$$

where $S_m$ is the scattering matrix at $m$-th interface which is defined as

$$\mathbf{S}_m = \begin{pmatrix} e^{-jk_{z,m} d_m} & e^{jk_{z,m} d_m} \\ -e^{-jk_{z,m} d_m} & e^{jk_{z,m} d_m} \end{pmatrix}^{-1} \begin{pmatrix} e^{-jk_{z,m-1} d_m} & e^{jk_{z,m-1} d_m} \\ -\frac{k_{z,m-1}}{k_{z,m}} e^{-jk_{z,m-1} d_m} & \frac{k_{z,m-1}}{k_{z,m}} e^{jk_{z,m-1} d_m} \end{pmatrix}. \quad (17)$$

where $d_m$ is a thickness of $m$-th plasma layer.

At the boundary between last plasma layer and free space (i.e. $z$=$z_T$), we obtain as following

$$\begin{pmatrix} B_n \\ C_n \end{pmatrix} = \mathbf{V}_T t, \quad (18)$$

where

$$\mathbf{V}_T = \begin{pmatrix} e^{-jk_{z,N} d_N} & e^{jk_{z,N} d_N} \\ -e^{-jk_{z,N} d_N} & e^{jk_{z,N} d_N} \end{pmatrix}^{-1} \begin{pmatrix} e^{-jk_{z,N+1} d_N} \\ -\frac{k_{z,N+1}}{k_{z,N}} e^{-jk_{z,N+1} d_N} \end{pmatrix}. \quad (19)$$

Combining Eqs. (14) and (16) with Eq. (18), we can obtain following:

$$\mathbf{S}_g \begin{pmatrix} r \\ 1 \end{pmatrix} = \mathbf{V}_T t, \quad (20)$$

where, $S_g$ is a global scattering matrix given by:

$$\mathbf{S}_g = \prod_{i=n}^{1} \mathbf{S}_i = \left( \mathbf{S}_{g1} \quad \mathbf{S}_{g2} \right). \quad (21)$$

where $S_{g1}$ and $S_{g2}$ represent the first and last column vectors of the matrix $S_g$. Then, the equation (20) can be transformed into

$$\begin{pmatrix} r \\ t \end{pmatrix}_{\mathbf{S}_g} = -\left( \mathbf{S}_{g1} - \mathbf{V}_T \right)^{-1} \mathbf{S}_{g2} \quad (22)$$

Finally, the power coefficients of reflection, transmission and absorption are expressed as follows:

$$R = |r|^2, \quad T = |t|^2, \text{ and } A = 1 - R - T \quad (23)$$

To see the propagation properties clearly of TE wave, we define the reflectance, transmittance and absorptance, respectively, by using the decibel scale as

$$\begin{aligned} Reflectance &= 20 \lg R, \\ Transmittance &= 20 \lg T, \\ Absorptance &= 20 \lg A \end{aligned} \quad (24)$$

## 2.3. Validity and Precision of SMM

In order to check the accuracy of this method, we compare SMM with DFDM [17] and approach of Wentzel-Kramers-Brillouin (WKB). Figure 3 shows the effect of the electron-neutral collision frequency on the propagation properties of a normally incident TE wave. In this calculation, a bell-like plasma-density distribution is assumed across the plasma layer in the $z$-direction $Ne(z)=Ne_{peak}[1-(1-2z/z_T)^2]^2$, where $Ne_{peak}=\omega^2 m_e \varepsilon_0/e^2$, the EM wave frequency is 2.85GHz, and the thickness of the plasma layer is taken as $z_T$=10cm. In Figure 4, we compare the transmittance results of SMM and WKB. Here the electron density distribution of plasma sheath is represented by a bi-Gaussian function as Eq. (1), where $Ne_{peak}=5\times10^{17}\text{m}^{-3}$, $a_1=a_2=5\text{m}^{-1}$, $z_T$=10cm, the collision frequency is $\nu$=20GHz, and the incident angle is $\theta=\pi/4$. As shown Figure 3 and Figure 4, it is seen apparently that the propagation properties calculated by using SMM is in a very good agreement in both DFDM and WKB. Therefore, we can apply the SMM to more complex calculations.

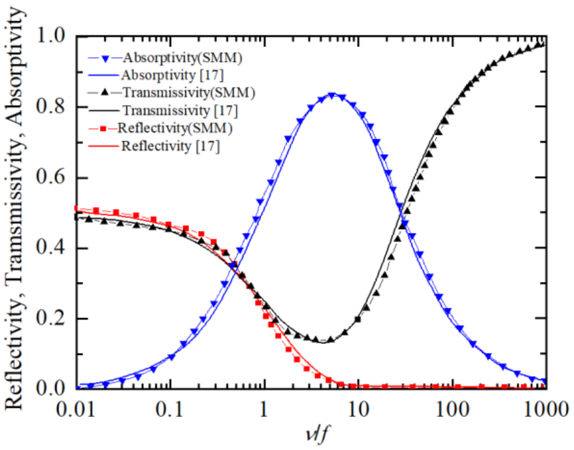


***Figure 3.*** *Comparison of SMM and DFDM for plasma sheath with bell-like density distribution.*

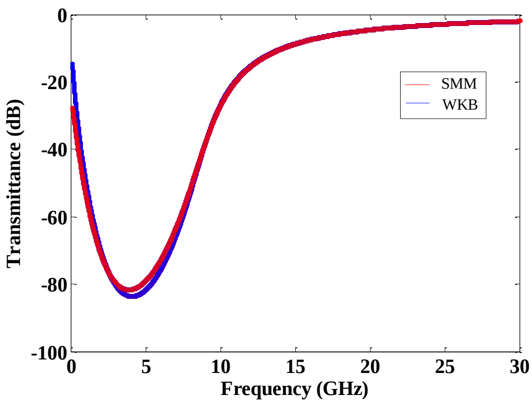


***Figure 4.*** *Comparison of SMM and WKB for plasma sheath with bi-Gaussian distribution.*

## 3. Numerical Results and Discussion

In this section, we calculate and discuss the effects of the reentry plasma sheath on the reflection, transmission, and absorption properties of the obliquely incident TE wave by using SMM. In our model, with respect to the typical reentry plasma sheath generated in the RAM-C project [25], the parameters range of the plasma sheath with a bi-Gaussian distribution is defined as $Ne_{peak}=10^{16}\text{m}^{-3}\sim10^{18}\text{m}^{-3}$, $\nu$=1GHz~80GHz, and $z_T$=10cm, respectively. The limit of incident angles $\theta$ of TE wave is set as 0 to $\pi/2$. To simplify the problem, the raise index $a_1$ and the fall-off index $a_2$ are both set to $5\text{m}^{-1}$, and the position of $Ne_{peak}$ is fixed at the center of the reentry plasma sheath. In order to evaluate the propagation properties of TE wave in the reentry plasma sheath, the nonuniform plasma sheath is divided into 50 thin layers with constant electron number density in each layer. The incident waveband is set from 1 GHz to 30GHz. The chosen frequency band covers the most common frequencies used in radar for L-, S-, C-, X-, Ku-, K-, and Ka-bands. The numerical results are shown below.

### 3.1. Influence of Incident Angle

Figure 5a-c show the reflectance, transmittance, and absorptance versus wave frequency and incident angle. Here, the maximum electron density and the collision frequency are $Ne_{peak}=5\times10^{17}\text{m}^{-3}$ and $\nu$=20GHz, respectively. In Figure 5a, the reflectance of TE wave in plasma sheath decreases with increasing the wave frequency, and increases with increasing the incident angle. Given incident angle, the Reflectance starts vibrating around 10GHz and the amplitude increases with increasing the frequency, and the larger the incident angle at same frequency, the smaller the amplitude. As shown in Figure 5b, at the same incident angle, the transmittance decreases as the frequency increases, reaching a minimum at a certain frequency, and then again increases. At a given frequency, the transmittance decreases gradually with increasing incident angle, and then a rapid decrease occurs at a certain angle. The minimum transmittances in Figure 5b and their corresponding frequencies and incident angles are listed in Table 1. As seen from Figure 5b and Table 1, the minimum transmittance decreases from with increasing the incident angle, and the frequency shifts from 3.13GHz to 9.59GHz towards high.

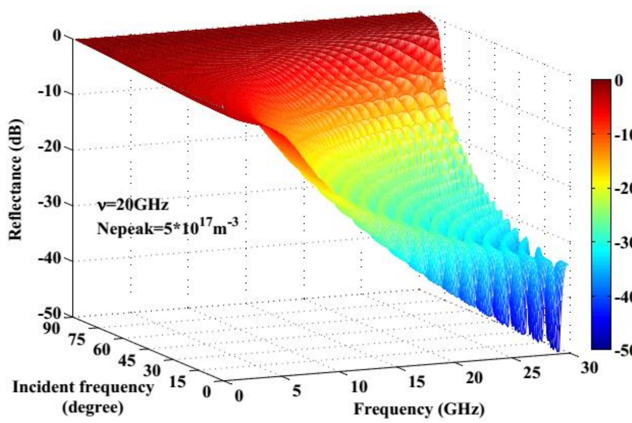


(a)

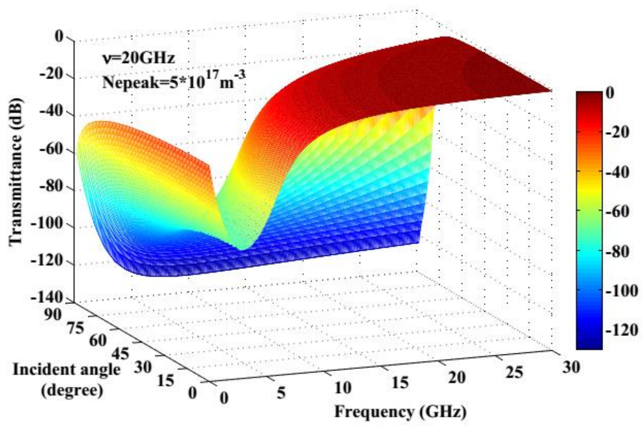


(b)

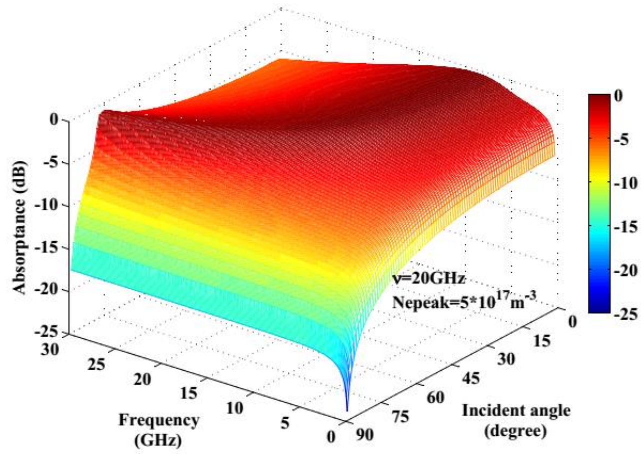


(c)

***Figure 5.*** *Dependence of (a) reflectance, (b) transmittance, and (c) absorptance for wave frequency and incident angles. The parameters are $Ne_{peak}=5\times10^{17}m^{-3}$ and $\nu$=20GHz.*

***Table 1.*** *Minimum transmittances in Figure 5b and their corresponding frequencies and incident angles. ($\nu$=20GHz, $Ne_{peak}=5\times10^{17}m^{-3}$).*

| Incident angle (degree) | Frequency (GHz) | Transmittance (dB) |
|---|---|---|
| 0 | 3.13 | -71.25 |
| 15 | 3.21 | -72.36 |
| 30 | 3.41 | -75.75 |
| 35 | 3.64 | -77.39 |
| 45 | 3.92 | -81.61 |
| 60 | 4.74 | -90.29 |
| 75 | 6.20 | -102.6 |
| 89 | 9.59 | -130.1 |

***Table 2.*** *Absorptance peaks in Figure 5c and their corresponding frequencies and incident angles. ($\nu$=20GHz, $Ne_{peak}=5\times10^{17}m^{-3}$).*

| Incident angle (degree) | Frequency (GHz) | Absorptance (dB) |
|---|---|---|
| 0 | 8.66 | -0.179 |
| 15 | 8.89 | -0.186 |
| 30 | 9.87 | -0.210 |
| 45 | 11.77 | -0.270 |
| 60 | 15.49 | -0.396 |
| 75 | 30 | -0.864 |

Figure 5c shows that, at given the incident angle, the absorptance increases with increasing frequency, reaches a peak at a certain frequency, and then decreases gradually.

The absorptance peaks in Figure 5c and their corresponding frequencies and incident angles is listed in Table 2. Figure 5c and Table 2 show that the absorptance peaks are formed at certain frequencies and incident angles, and with increasing incident angle, the absorptance peak gradually decreases and shifts from low to high frequencies.

## 3.2. Influence of Maximum Electron Density

In order to investigate the effects on the reflection, transmission, and absorptance properties of the obliquely incident TE wave for the maximum electron density in our model, we fix the collision frequency and the incident angle to $\nu$=20GHz and $\theta=\pi/3$, respectively. Figure 6a-c exhibit the reflectance, transmittance, and absorptance of obliquely incident TE wave versus wave frequency for various maximum electron density of plasma, where blue, red, and black lines represent the maximum electron densities $Ne_{peak}=10^{16}m^{-3}$, $Ne_{peak}=10^{17}m^{-3}$, and $Ne_{peak}=10^{18}m^{-3}$, respectively. Figure 6a shows that the reflectance decreases with increasing the wave frequency, and increases with increasing the maximum electron density. As shown in Figure 6b, the transmittance depend strongly on the maximum electron density of the plasma, the minimum transmittances decrease rapidly such as -3.9dB, -29.3dB, and -138.0dB for the maximum electron density $Ne_{peak}=10^{16}m^{-3}$, $Ne_{peak}=10^{17}m^{-3}$, and $Ne_{peak}=10^{18}m^{-3}$, respectively. In addition, with increasing the maximum electron density, the transmittance peak shifts from 1.3GHz to 5.8GHz, and is broadened. The absorptance increases with increasing the maximum electron density, and the absorptance peak values are respectively -2.71dB, -0.49dB, and -0,41dB for the maximum electron density $Ne_{peak}=10^{16}$GHz, $Ne_{peak}=10^{17}$GHz, and $Ne_{peak}=10^{18}$GHz, as shown in Figure 6c. From the figure, we can also see that the absorptivity bands are broaded, and the absorptance peaks shift to the higher frequency range such as 1.8GHz, 6.45GHz, and 23.14GHz, as the electron densities are enhanced.

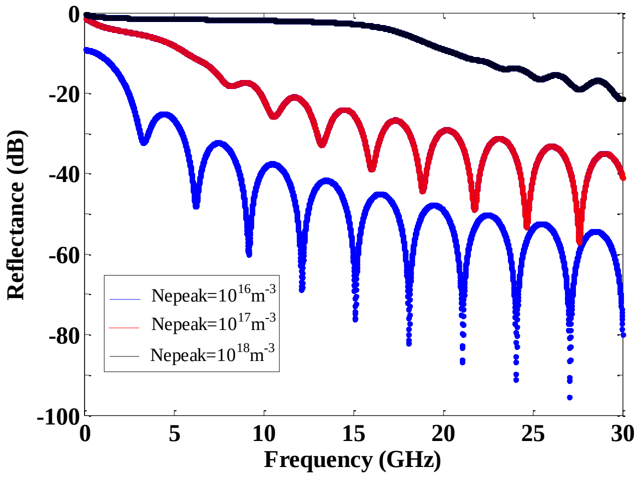


(a)

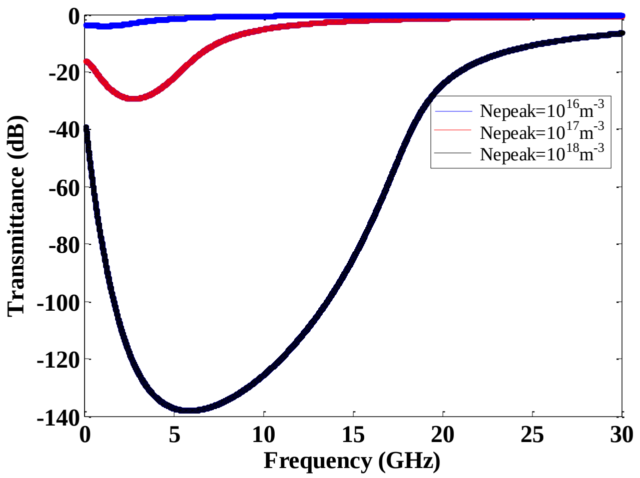


(b)

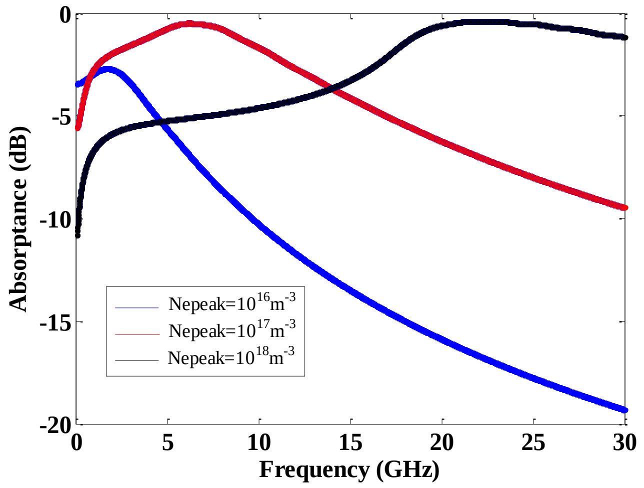


(c)

***Figure 6.*** *Dependence of (a) reflectance, (b) transmittance, and (c) absorptance on wave frequency for various maximum electron densities. The parameters are* $\nu$*=20GHz and* $\theta=\pi/3$.

### 3.3. Influence of Collision Frequency

Figure 7a-c show the reflectance, transmittance, and absorptance versus wave frequency and collision frequency. Here, the maximum electron density and incident angle are $Ne_{peak}=10^{18}m^{-3}$ and $\theta=\pi/6$, respectively. As shown Figure 7a, the reflectance decreases and vibrates with increasing the wave frequency and collision frequency, but the variation with the collision frequency is not so severe. Figure 7b shows that the transmittance decreases and then increases again with increasing frequency, and increases at low frequencies, but decreases slightly at high frequencies, with increasing collision frequency. The minimum transmittance increases with increasing collision frequency such as -170.2dB, -120.5dB, -91.5dB, -71.9dB, and -55.7dB, for the collision frequency 1GHz, 20GHz, 40GHz, 60GHz, and 80GHz, respectively. In addition, the minimum transmittance point shifts from 4.9GHz to 7.3GHz with increasing the collision frequency.

Figure 7c shows that the absorptance increases with increasing the collision frequency, and at high frequency and high collision frequency, the most of TE wave are absorbed. It is because the higher the collision frequency, the more frequent the collision between electrons and neutral particles, and the greater the momentum transfer from electrons to neutral particles, thus increasing the absorption energy.

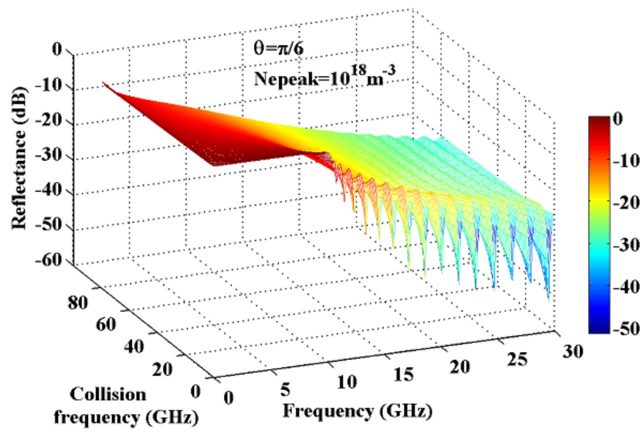


(a)

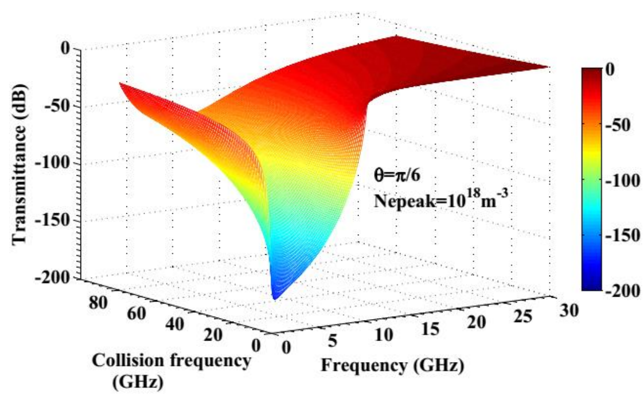


(b)

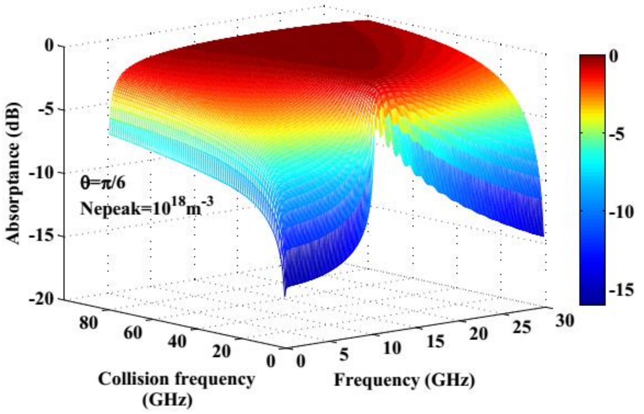


(c)

***Figure 7.*** *Dependence of (a) reflectance, (b) transmittance, and (c) absorptance for wave frequency and collision frequency: The parameters are* $Ne_{peak}=10^{18}m^{-3}$ *and* $\theta=\pi/6$.

## 4. Conclusion

The calculation results show that the larger the angle of incidence in the wide frequency band, the greater the reflectance but the lower the transmittance, and the absorptance decreases monotonically with increasing incident angle below a certain frequency, but at higher frequencies the absorbance peak appears and this absorbance peak shifts towards higher frequencies. The plasma electron density has a great influence on the propagation characteristics of TE waves. That is, when the maximum electron density of the plasma layer is increased, the reflectance and absorptance increase greatly, whereas the transmittance decreases rapidly, and the transmittance decreases less than -30 dB in the wide range from 1 GHz to 18 GHz as the maximum electron density is $Ne_{peak}=10^{16}m^{-3}\sim10^{18}m^{-3}$. As the collision frequency increases, the reflectance decreases slightly, but the transmittance and absorptance increase. In particular, in plasma sheath with high collision frequencies, most of the TE waves can be absorbed. Our approach can be applied to the study of the propagation characteristics of electromagnetic waves obliquely incident with arbitrary frequency into the plasma. These results can be useful for the research on the communication blackout in the reentry plasma sheath.

## Abbreviations

| | |
|---|---|
| EM | Electromagnetic |
| SMM | Scattering Matrix Method |
| DFDM | Direct Finite-Difference Method |
| WKB | Wentzel-Kramers-Brillouin |

## Acknowledgments

Authors thank Prof. Yong-Jun Kim for useful advice.

## Author Contributions

**Chol-Su Kim:** Formal Analysis, Investigation, Methodology, Software, Visualization, Writing – original draft
**Yong-Su Han:** Formal Analysis, Investigation, Methodology, Supervision, Writing – review & editing
**Myong-Il Ri:** Resources, Software, Supervision, Validation
**Il-Guk Kim:** Conceptualization, Data curation, Validation
**Se-Chol Pak:** Validation, Writing – review & editing

## Funding

This work is not supported by any external funding.

## Data Availability Statement

The data is available from the corresponding author upon reasonable request.

## Conflicts of Interest

The authors declare no conflicts of interest.

## References

[1] Rybak, J. P., Churchill, R. J., Progress in reentry communications, IEEE Trans. Aerosp. Electron. Syst., 1971, AES-7(5), 879–894.

[2] Hartunian, R. A., Stewart, G. E., Fergason, S. D., Curtiss, T. J., Seibold, R. W., Causes and mitigation of radio frequency (RF) blackout during reentry of reusable launch vehicles, Aerospace Corporation, El Segundo, CA, USA, Contractor Rep. ATR–2007(5309)–1.

[3] R. L. Stenzel and J. M. Urrutia, A new method for removing the blackout problem on reentry vehicles, J. Appl. Phys. vol. 113, pp. 103303(1–5), 2013, https://doi.org/10.1063/1.4795148

[4] G. Wei, C. Yan, P. Chen, Z. Zhang, Q. Nie and X. Ai, Transmission and Scattering Characteristics in Plasma Sheaths of Re-Entry Vehicles Due to Multieffect Synergy, IEEE Trans. Antennas Propag., 2023, 71(3), https://doi.org/10.1109/TAP.2022.3231056

[5] Wei, G., Yanpeng, H., Fangfang, S., Peng, X., Polarization Characteristics Distortion for L-Band Fully polarimetric Radar Subject to Magnetized Plasma Sheath, Remote Sensing, 2024, 16(12), https://doi.org/10.3390/rs16122061

[6] Tang, D. L., Sun, A. P., Qiu, X. M., Chu, P. K., Interaction of electromagnetic waves with a magnetized nonuniform plasma slab, IEEE Trans. Plasma Sci. 2003, 31(3), 405–410, https://doi.org/10.1109/TPS.2003.811648

[7] Gürel, Ç. S., Öncü, E., Interaction of electromagnetic wave and plasma slab with partially linear and sinusoidal electron density profile, Prog. Electromagn. Res. Letter, 2009, 12, 171–181.

[8] Yuan, C. X., Zhou, Z. X., Sun, H. G., Reflection Properties of Electromagnetic Wave in a Bounded Plasma Slab, IEEE Trans. Plasma Sci., 2010, 38(12), 3348–3355, https://doi.org/10.1109/TPS.2010.2084110

[9] Yuan, C. X., Zhou, Z. X., Xiang, X. L., Sun, H. G., Wang, H., Xing, M. D., Luo, Z. J., Propagation properties of broadband terahertz pulses through a bounded magnetized thermal plasma, Nuclear Instruments and Methods in Physics Research B, 2011, 269(1), 23–29, https://doi.org/10.1016/j.nimb.2010.10.003

[10] Hu, B. J., Wei, G., Lai, S. L., SMM analysis of reflection, absorption and transmission from nonuniform magnetized plasma slab, IEEE Trans. Plasma Sci., 1999, 27(4), 1131–1136.

[11] Luís, D., Giangaspero, V., Viladegut, A., Lani, A., et al. Effect of electron number densities on the radio signal propagation in an inductively coupled plasma facility, Elsevier Ltd, Acta Astronautica, 2023, 212, https://doi.org/10.1016/j.actaastro.2023.07.028

[12] Gregoire, D. J., Santoru, J., Schumacher, R. W., Electromagnetic wave propagation in unmagnetized plasmas, Hughes Res. Labs, Malibu, CA, 1992, AD–A250710.

[13] Cao, J., Li, J., Chen, G., Absorption characteristics of conductive targets coated with plasma, Chin. J. Radio Sci., 2002, 17(2), 125–128.

[14] Ji, J. Z., Ma, Y. P., Guo, N., Numerical calculation of the reflection, absorption and transmission of a nonuniform plasma slab based on FDTD, Optik, 2018, 165, 240–247, https://doi.org/10.1016/j.ijleo.2018.03.118

[15] Sun, S. B., Liu, S., Zhong, S. Y., Analysis of terahertz wave penetration capacity to 2D conductive cylinder coated with steady-state parabolic distribution plasma media, Results in Physics. 2021, 27, 104516, https://doi.org/10.1016/j.rinp.2021.104516

[16] Laroussi, M., Roth, J. R., Numerical calculation of the reflection, absorption, and transmission of microwaves by a nonuniform plasma slab, IEEE Trans. Plasma Sci., 1993, 21(4), 366–372, https://doi.org/10.1016/j.ijleo.2011.04.015

[17] Cheng, G. X., Liu, L., Direct finite-difference analysis of the electromagnetic-wave propagation in inhomogeneous plasma, IEEE Trans. Plasma Sci., 2010, 38(11), 3109–3115, https://doi.org/10.1109/TPS.2010.2071886

[18] Bai, B. W., Li, X. P, Liu, Y. M., Xu, J., Shi, L., Xie, K., Effects of reentry plasma sheath on the polarization properties of obliquely incident EM waves, IEEE Trans. Plasma Sci. 2014, 42(10), 3365–3372, https://doi.org/10.1109/TPS.2014.2349009

[19] Mao, M., Peng K., Zhao, Z., Yuan, K., Xiong, J., Tang, R., Deng, X., Modeling and Analysis on Dynamic Terahertz Channel Capacity in Hypersonic Plasma Sheaths, IEEE Trans. Plasma Sci. 2024, 52(2), https://doi.org/10.1109/TPS.2024.3369104

[20] Swift, C. T., Beck, F. B., et al., RAM C-III S-Band Diagnostic Experiment: The Entry Plasma Sheath and Its Effects on Space Vehicle Electromagnetic Systems, NASA Langley Research Center, Hampton, Virginia, 1970, 1, 137–156.

[21] Rawhouser, R., Overview of the AF Avionics Laboratory reentry electromagnetics program, NASA, Washington, DC, USA, Tech. Rep. NASA/SP–252, 1971.

[22] He, G. L., Zhan, Y. F., Zhang, J. Z., Ge, N., Characterization of the Dynamic Effects of the Reentry Plasma Sheath on Electromagnetic Wave Propagation, IEEE Trans. Plasma Sci..2016, 44(3), 232–238, https://doi.org/10.1109/TPS.2016.2517159

[23] Ginzburg, V. L., The Propagation of Electromagnetic Waves in Plasmas, Pergamon, New York, 1970, 118.

[24] Chew, W. C., Waves and Fields in Inhomogeneous Media, Van Nostrand Reinhold, New York, 1990, 45.

[25] Dix, D. M., Typical values of plasma parameters around a conical re-entry vehicle, Aerospace Corporation, El Segundo, CA, USA, Sci. Rep. 1962, AD295429.